molecular pharmaceutics

Article

pubs.acs.org/molecularpharmaceutics

Highly Efficient One-Pot Labeling of New Phosphonium Cations with Fluorine-18 as Potential PET Agents for Myocardial Perfusion Imaging

Zuoquan Zhao,[†,‡] Qian Yu,[†] Tiantian Mou,[†] Chang Liu,[†,§] Wenjiang Yang,[∥] Wei Fang,[⊥] Cheng Peng,[#] Jie Lu,[†] Yu Liu,[∥] and Xianzhong Zhang*[,§]

[†]Key Laboratory of Radiopharmaceuticals, Ministry of Education, College of Chemistry, Beijing Normal University, 19 Xinjiekou Outer Street, Beijing 100875, China

[§]Center for Molecular Imaging and Translational Medicine, State Key Laboratory of Molecular Vaccinology and Molecular Diagnostics, School of Public Health, Xiamen University, Xiang'an South Road, Xiamen 361102, China

[⊥]Department of Nuclear Medicine, Cardiovascular Institute and FuWai Hospital, Chinese Academy of Medical Sciences, Beijing 100037, China

[∥]Key Laboratory of Nuclear Radiation and Nuclear Energy Technology, Institute of High Energy Physics, Chinese Academy of Sciences, Beijing 100049, China

[#]PET Center of Xuanwu Hospital, Capital Medical University, Beijing 100053, China

Supporting Information

ABSTRACT: Lipophilic cations such as phosphonium salts can accumulate in mitochondria of heart in response to the negative inner-transmembrane potentials. Two phosphonium salts [^{18}F]FMBTP and [^{18}F]mFMBTP were prepared and evaluated as potential myocardial perfusion imaging (MPI) agents in this study. The cations were radiolabeled via a simplified one-pot method starting from [^{18}F]fluoride and followed by physicochemical property tests, *in vitro* cellular uptake assay, *ex vivo* mouse biodistribution, and *in vivo* rat microPET imaging. The total radiosynthesis time was less than 60 min including HPLC purification. The [^{18}F] labeled compounds were obtained in high radiolabeling yield (~50%) and good radiochemical purity (>99%). Both compounds were electropositive, and their log *P* values at pH 7.4 were 1.16 ± 0.003 (n = 3) and 1.05 ± 0.01 (n = 3), respectively. Both [^{18}F]FMBTP and [^{18}F]mFMBTP had high heart uptake (25.24 ± 2.97% ID/g and 31.02 ± 0.33% ID/g at 5 min postinjection (p.i.)) in mice with good retention (28.99 ± 3.54% ID/g and 26.82 ± 3.46% ID/g at 120 min p.i.). From the PET images in rats, the cations exhibited high myocardium uptake and fast clearance from liver and small intestine to give high-contrast images across all time points. These phosphonium cations were radiosynthesized via a highly efficient one-pot procedure for potential MPI offering high heart accumulation and rapid nontarget clearance.

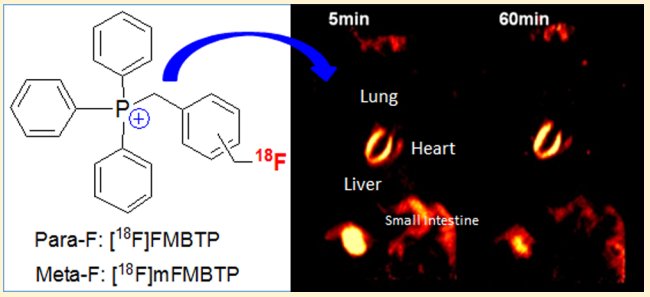

KEYWORDS: *^{18}F-labeled phosphonium cation, one-pot radiosynthesis, positron emission tomography, biodistribution, myocardial perfusion imaging agent*

INTRODUCTION

MPI is the most important noninvasive method in the diagnosis and treatment of coronary heart disease (CAD).[1] Desired agent for MPI should have the following properties: (1) rapid clearance from blood; (2) quick myocardial uptake and high myocardial uptake rate; (3) satisfactory heart-to-blood, heart-to-liver, and heart-to-lung ratios. Currently, single-photon emission computed tomography (SPECT) imaging with [^{99m}Tc]sestamibi has been used as the gold standard of MPI in nuclear medicine for decades.[1−4] However, the technical limitations of SPECT imaging, such as low spatial resolution, lack of effective methods of tissue attenuation correction, and the high uptake in organs near the heart may compromise the delineation of small infarcts and the diagnostic accuracy.[4,5]

Positron emission tomography (PET) has several technical advantages compared with SPECT.[6,7] But the half-life of currently used PET tracers for MPI is too short, for example [^{13}N]ammonia ($t_{1/2}$ = 10 min), [^{82}Rb]rubidium ($t_{1/2}$ = 75 s),

Special Issue: Positron Emission Tomography: State of the Art

Received: March 23, 2014
Revised: May 9, 2014
Accepted: May 22, 2014
Published: May 22, 2014

Scheme 1. $^{18}F/^{11}C$-Labeled Analogues of Mitochondrial Complex I Inhibitor As Potential MPI Agents

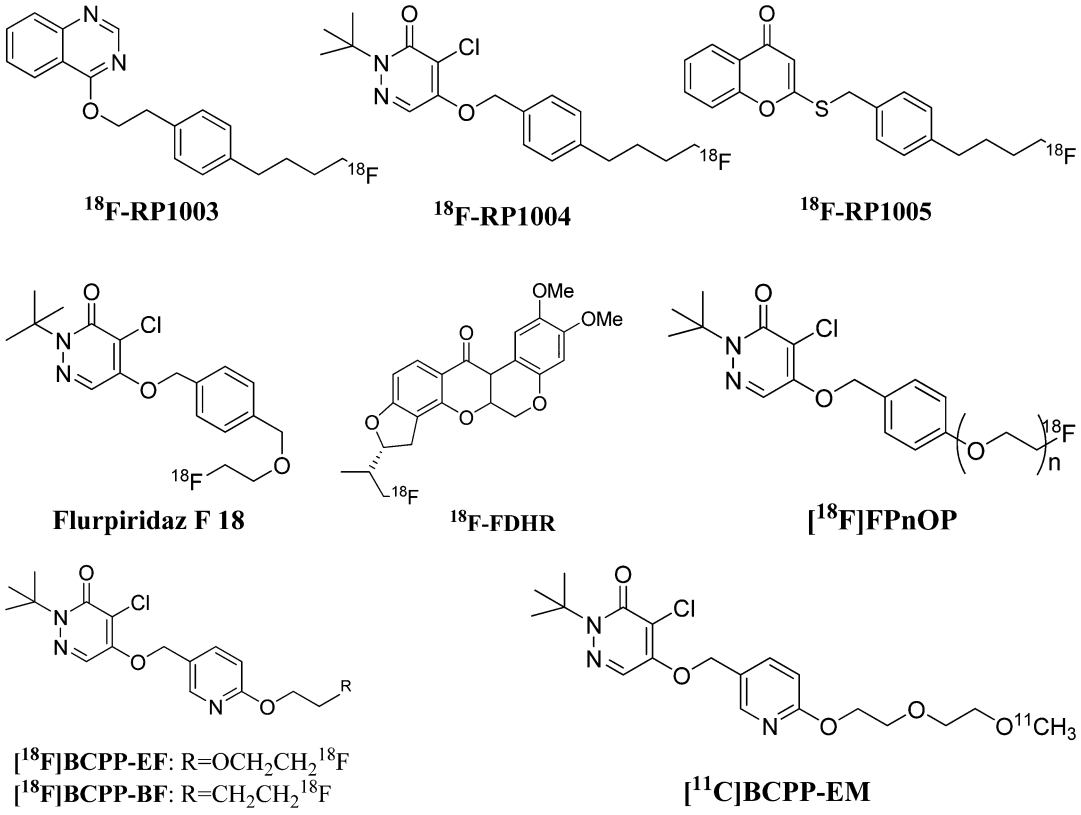

Scheme 2. ^{18}F-Labeled Lipophilic Phosphonium Cations As Potential MPI Agents

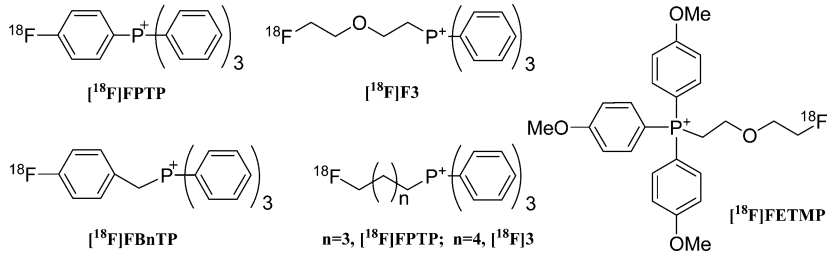

and [^{15}O]water ($t_{1/2}$ = 2 min), which limits their widespread clinical use.[8−10] [^{18}F]Fluoride has an appropriate physical half-life ($t_{1/2}$ = 110 min), good biocompatibility, and an atomic radius similar to that of the hydrogen atom.[2,11] Therefore, the development of novel ^{18}F-labeled myocardial perfusion imaging agents has become a research of interest in recent years. In the previous studies, we and other research groups reported several $^{18}F/^{11}C$-labeled analogues of mitochondrial complex I (MC-I) inhibitors (Scheme 1) as potential MPI agents.[2,3,12,13] Most of those compounds have much better image quality and relationship to myocardial blood flow than that of [^{99m}Tc]-sestamibi.[14,15]

Other kinds of ^{18}F-labeled compounds of lipophilic cations (Scheme 2), which can target mitochondria via a membrane potential dependent mechanism in cardiomyocytes,[16−19] were also developed as potential MPI agents.[1,20−23] They are accumulated to the heart via a mechanism similar to that of the technetium complexes ([^{99m}Tc]sestamibi and [^{99m}Tc]-tetrofosmin) and exhibit high myocardium uptake. Unfortunately, the time-consuming multiple-step radiolabeling procedure,[1] low radiolabeling yield,[1,20,21] and unfavorable hepatic clearance[23] limited their further study and use in clinic. Therefore, it is meaningful to develop a more effective labeling method for preparing ^{18}F-labeled phosphonium cations with favorable liver clearance.

In this article, two novel phosphonium cations, [^{18}F]4-(fluoromethyl)benzyltriphenyl phosphonium ([^{18}F]FMBTP) and [^{18}F](3-(fluoromethyl)benzyl)trisphenyl phosphonium ([^{18}F]mFMBTP), were synthesized by using a simple one-pot procedure with high labeling yield in a short synthesis time. *In vitro* cellular uptake assay, *ex vivo* biodistribution study in mice, and *in vivo* microPET imaging in rats were carried out to evaluate their biological properties as potential MPI agents.

EXPERIMENTAL SECTION

Materials. [^{18}F]Fluoride was obtained from PET Center of Xuanwu Hospital (Beijing, China). Other reagents and solvents were purchased from commercial suppliers. Paper electrophoresis experiments were carried out using 0.025 mol/L phosphate buffer (pH 7.4) and Xinhua 1# filter paper at 150 V for 180 min. Reversed-phase high-pressure liquid chromatography (RP-HPLC) was performed on an SHIMADZU system

dx.doi.org/10.1021/mp500216g | *Mol. Pharmaceutics* 2014, 11, 3823−3831

with LC-20AT pump and B-FC-3200 BIOSCAN flow-counter. The C-18 reverse-phase semipreparative HPLC column (10 × 250 mm, 5 μm particle size, Venusil MP-C18, Agela Technologies Inc., USA) was eluted at a flow rate of 5 mL/min. Labgen 7 homogenizer was purchased from Cole-Parmer Instrument Co (USA). ^{1}H NMR spectra were recorded on a Bruker (400 MHz) spectrometer. Mass spectra were recorded using a Bruker Compass Data analysis 4.0. Chemical shifts are reported in δ (ppm) values.

Kunming mice (18−20 g) and Spraque-Dawley rats (250−260 g) were obtained from the Animal Center of Peking University. Beagle dogs were obtained from the Beijing Rixin Technology Co., Ltd. All biodistribution studies were performed under a protocol approved by Beijing Administration Office of Laboratory Animal (BAOLA).

Chemistry: Synthesis of Nonradioactive Reference Compounds. 4-(Fluoromethyl)benzyltriphenyl phosphonium ([^{19}F]FMBTP) and 3-(fluoromethyl)benzyltriphenyl phosphonium ([^{19}F]mFMBTP) were synthesized as reference compounds with similar two-step procedure.

tert-Butylammonium fluoride (TBAF, 6 mmol) and acetonitrile (anhydrous, 5 mL) were placed into a three-necked flask (100 mL), and the liquid was evaporated at 110 °C under a stream of nitrogen. Two azeotropic evaporations with acetonitrile (anhydrous, 2 × 5 mL) were carried out at 110 °C under a stream of nitrogen, and 1,4-bis(bromomethyl)-benzene (1.32 g, 5 mmol) in acetonitrile (anhydrous, 30 mL) was added at 60 °C. The mixture was kept at 100 °C overnight and concentrated. [^{19}F]BMFMB was obtained as a colorless oil (0.4 g, 40%) after silica gel chromatography (mineral ether). [^{19}F]mBMFMB was obtained as a colorless oil (0.18 g, 45%) by using a procedure similar to that described above, except starting from 1,3-bis(bromomethyl)benzene (0.528 g, 2 mmol). [^{19}F]BMFMB and [^{19}F]mBMFMB were characterized by ^{1}H NMR and ^{19}F NMR (see Supporting Information).

[^{19}F]BMFMB or [^{19}F]mBMFMB (0.14 g, 0.7 mmol), triphenylphosphine (0.24 g, 0.9 mmol), and anhydrous acetonitrile (25 mL) were placed into a three-necked flask (100 mL) stirred at 85 °C for 5 h. After cooled to room temperature, the reactant was concentrated under reduced pressure. After that, [^{19}F]FMBTP was obtained as a white solid (0.11 g, 35%) after eluted with the mixture of ethyl acetate and petroleum ether =1:1 (v/v). While for [^{19}F]mFMBTP, it was obtained as a white solid (0.1 g, 32%) after silica gel chromatography (CH_2Cl_2 /CH_3OH = 20:1 (v/v)). ^{1}H NMR and ^{19}F NMR for [^{19}F]FMBTP: ^{1}H NMR (400 MHz, $CDCl_3$) δ: 5.22 (s,1H), 5.34 (s,1H)), 5.46 (d,2H), 7.12−7.17 (m, 4H), 7.16−7.65 (m, 15H); ^{19}F NMR (400 MHz, $CDCl_3$) δ: −208.35; HRMS: m/z[M$^+$] calculated for [^{19}F]FMBTP: 385.1516, found 385.1175. ^{1}H NMR and ^{19}F NMR for [^{19}F]mFMBTP: ^{1}H NMR (400 MHz, $CDCl_3$) δ: 5.09 (s,1H)), 5.21 (s,1H)), 5.51 (d,2H), 7.17−7.24 (m, 4H), 7.62−7.64 (m, 15H); ^{19}F NMR (400 MHz, $CDCl_3$) δ: −208.27; HRMS: m/z[M$^+$] calculated for [^{19}F]mFMBTP: 385.1516, found 385.1511.

Radiochemistry. *Preparation of [^{18}F]BMFMB and [^{18}F]-mBMFMB.* The labeling procedure of [^{18}F]BMFMB (or [^{18}F]mBMFMB) is similar to that of published previously.[24,25] While in our study, the amount of reagents were modified to obtain high radiochemical yields (see Supporting Information). Briefly, after the solvent of [^{18}F]fluoride eluate (1.5 mg of K_2CO_3 in 0.3 mL of H_2O and 2 mg of Kryptofix 2.2.2 in 1 mL of acetonitrile) was evaporated under a stream of nitrogen at 110 °C, the extra anhydrous acetonitrile (0.5 mL) was added three times, to remove the residual water. After that, 1,4-bis(bromomethyl)benzene (for [^{18}F]BMFMB) or 1,3-bis-(bromomethyl)benzene (for [^{18}F]mBMFMB) was dissolved in anhydrous acetonitrile (3 mg in 0.5 mL) and added to the residuals. After vibrating at 100 °C for 6 min, the reaction mixture was cooled to room temperature. The crude product could be used for next step without further purification. The radiochemical yields were calculated by analytical HPLC. The column was eluted with water (solvent A) and acetonitrile (solvent B) at a flow rate of 1.0 mL/min (gradient method). Gradient: 0−3 min, 95−60% A; 3.01−7 min, 60−30% A; 7.01−20 min, 0% A.

Preparation of [^{18}F]FMBTP and [^{18}F]mFMBTP. Triphenylphosphine (5 mg in 0.5 mL of anhydrous acetonitrile) was added to the unpurified crude ([^{18}F]BMFMB or [^{18}F]-mBMFMB) and stirred at 90 °C for 15 min. After being cooled to room temperature, the final reactant was injected onto a semipreparative HPLC column for purification. The column was eluted with PBS (pH = 7, 0.02 mol/L) and acetonitrile (v/v = 1:1) at a flow rate of 3.0 mL/min (isocratic purification method). The appropriate fraction was collected and evaporated to remove acetonitrile, and then the activity was reconstituted in phosphate-buffered saline and passed through a 0.22 μm Millipore filter into a sterile vial for *in vivo* applications. The radiochemical purity was assayed by analytical HPLC by using PBS (pH = 7, 0.02 mol/L) and acetonitrile (v/v = 1:1) at a flow rate of 1.0 mL/min (isocratic analysis method).

Physicochemical Property Studies. The octanol/water partition coefficient was measured following 5−8 min of vigorous vortex mixing of 600 μL of *n*-octanol and 600 μL of phosphate buffer (0.025 mol/L, pH 7.4) with [^{18}F]FMBTP or [^{18}F]mFMBTP in a tube. The tube was centrifuged at 14000 rpm for 5 min, and the counts in 500 μL aliquots of both organic and aqueous layers were determined. Then the organic and aqueous phases were mixed again, and the above operation was repeated three times to ensure that the ratio of counts in organic and aqueous phases remained unchanged. The partition coefficient (P) was calculated using the following equation: P = (cpm in the organic phase − background cpm)/(cpm in the aqueous phase − background cpm). The partition coefficient value was expressed as log P.

For paper electrophoresis experiments, the radiotracer ([^{18}F]FMBTP or [^{18}F]mFMBTP) was spotted on a chromatography paper strip (10 cm × 1 cm), which was pretreated with phosphate buffer (0.025 mol/L, pH = 7.4). The strip was developed in phosphate buffer (0.025 mol/L, pH = 7.4) at 150 V for 2 h. Then the radioactivity distribution of radiotracer on the strip was determined.

For *in vitro* stability study, radiotracer ([^{18}F]FMBTP or [^{18}F]mFMBTP) was incubated in 1 mL of water at room temperature or in 0.5 mL of murine plasma at 37 °C for 3 h, respectively. Plasma proteins were precipitated by adding 150 μL of acetonitrile and removed by centrifugation. The radiochemical purity was assayed by HPLC using the isocratic analysis method.

Cell Uptake Studies. The cell uptakes of lipophilic cations of [^{18}F]FMBTP and [^{18}F]mFMBTP were determined in rat embryonic cardiomyoblast cell line (H9c2) and mouse normal fibroblast cell line (NIH/3T3), respectively. All cells were grown in Dulbecco's modified Eagle medium high glucose (containing KCl, 5.3 mmol/L, and NaCl, 110.34 mmol/L), plus 10% fetal bovine serum and 1% penicillin−streptomycin at 37

°C in 5% CO_2 and 95% air. Twenty-four hours before the experiment, the H9c2 and NIH/3T3 cells were seeded in 48 well plates (0.05 M cell/well, 0.5 mL) and incubated at 37 °C to form confluent monolayers. After the radiotracer ([^{18}F]FMBTP or [^{18}F]mFMBTP, 18.5 kBq/100 μL) was added, cells were incubated at 37 °C for 1 h. Then the radioactive medium was removed, and the wells were washed two times with cold phosphate-buffered saline (0.01 mol/L; pH, 7.4; 0.2% BSA). The cells were lysed by treated with 0.5 mL of 1 mol/L NaOH for 5 min at room temperature and transferred to tubes, and the radioactivity was measured using a gamma counter. The cell uptakes of [^{99m}Tc]sestamibi (11.1 kBq/100 μL) in H9c2 and NIH/3T3 cells were also performed for comparison.

The mitochondrial membrane potential (MMP) dependent cellular uptake of radiotracers was further evaluated with H9c2 cells pretreated with carbonyl cyanide *m*-chlorophenylhydrazone (CCCP), which is a protonophore that selectively abolishes the mitochondrial membrane potential.[26] The radiotracer was dissolved in dimethyl sulfoxide and diluted to the desired concentration with low-K^+ HEPES buffer (NaCl, 135 mmol; KCl, 5 mmol/L; $CaCl_2$, 1.8 mmol/L; $MgSO_4$, 0.8 mmol/L; HEPES, 50 mmol/L; dextrose, 5.5 mmol/L; pH, 7.4).[27] The final concentration of dimethyl sulfoxide was <0.1%. CCCP solution (1 μM) was added to 5.0×10^4 cells for 30 min at 37 °C before the start of the experiment. After incubation with [^{18}F]FMBTP ([^{18}F]mFMBTP or [^{99m}Tc]-sestamibi), the cells were washed and lysed to count the radioactivity by a gamma counter.

***Ex Vivo* Biodistribution Studies.** About 185 kBq [^{18}F]FMBTP or [^{18}F]mFMBTP (0.1 mL) was injected through the tail vein of wild type Kunming mice (n = 5). The mice were sacrificed at 5, 30, 60, and 120 min after injection. The tissues and organs of interest were collected, wet weighed, and counted in gamma counter (WIZARD1470, PerkinElmer, USA). The percentage of injected dose per gram (% ID/g) for each sample was calculated by comparing its activity with appropriate standard of injected dose (ID), the values expressed as mean ± standard deviation (SD).

MicroPET Imaging in Rat. All the animal protocols were approved by the Institute's Animal Care and Use Committee. Normal male Spraque-Dawley rat (250−260 g) was anesthetized with isoflurane and placed near the center of the field of view of the PET scanner (Siemens Inveon). About 21 MBq of [^{18}F]mFMBTP was injected intravenously. Static PET scans were performed to evaluate myocardial uptake at 5, 30, 60, and 120 min after the tracer injection, and the each scan time was 10 min, respectively. Dynamic small-animal PET images were acquired for 120 min (6 s × 10 frames, 60 s × 4 frames, 300 s × 6 frames, 600 s × 9 frames) after injection. The images were reconstructed using a two-dimensional ordered-subsets expectation maximization (2-D OSEM) algorithm without attenuation or scattering correction. Three-dimensional regions of interests (3D-ROIs) were placed on for the ROI drawing.

PET/CT Imaging in Dog. Animal procedures were performed following National Institutes of Health guidelines and were approved by FuWai Hospital, Chinese Academy of Medical Science.

For the whole-body PET/CT study, a healthy Beagle dog (15 kg) was anesthetized by a mixture of ketamine (25 mg/kg) and diazepam (1.1 mg/kg). Anesthesia was supplemented as needed. The animal was placed prone on the PET/CT bed, and a venous catheter was established for radiotracer injection. About 55 MBq of [^{18}F]mFMBTP in 2 mL of saline solution was injected. Whole-body imaging was performed at 10, 30, 60, and 120 min after injection. PET data were acquired on a PET/CT system (Biograph 64, Siemens). Whole-body scanning involved 4 bed positions, with each scanned for 2 min. Regions of interest were drawn on the myocardium, liver, and lung. Standardized uptake value was calculated as [mean region-of-interest count (cps/pixel) × body weight (kg)]/[injected dose (mCi) × calibration factor (cps/pixel)]. The myocardium/liver and myocardium/lung standardized uptake value ratios at each time point were evaluated.

RESULTS

Chemistry. The intermediate products of [^{19}F]BMFMB and [^{19}F]mBMFMB were synthesized and characterized by ^{1}H NMR and ^{19}F NMR (see Supporting Information). Nonradioactive references [^{19}F]FMBTP and [^{19}F]mFMBTP were characterized by ^{1}H NMR, ^{19}F NMR and HRMS. The synthetic routes are shown in Figure 1. The chemical yields of

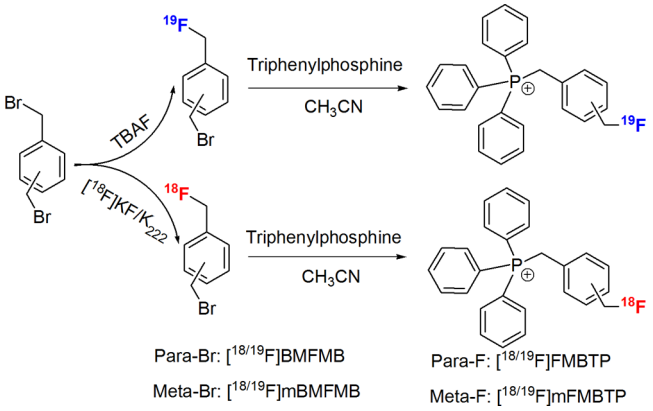

Figure 1. Synthetic routes of [$^{18/19}$F]FMBTP and [$^{18/19}$F]mFMBTP.

[^{19}F]BMFMB, [^{19}F]mBMFMB, [^{19}F]FMBTP, and [^{19}F]-mFMBTP were 40%, 45%, 35%, and 32%, respectively. The chemical purities of nonradioactive references [^{19}F]FMBTP and [^{19}F]mFMBTP were calculated as >98% from the HPLC chromatogram (λ = 254 nm) (see Supporting Information: Figure S1 and S2). Besides that, there is more than 2 min difference between the retention time of intermediates and final compound, meaning that the intermediates could be separated clearly from the final reference compounds.

Radiochemistry: Preparation of Radiointermediates. For the synthesis of [^{18}F]BMFMB, 1,4-bis(bromomethyl)-benzene was reacted with non-carrier-added [^{18}F]fluoride in the presence of Kryptofix 2.2.2 and K_2CO_3 (Figure 1). HPLC analysis revealed that the [^{18}F]BMFMB exhibited identical retention time with a fully characterized [^{19}F]BMFMB (see Supporting Information: Figure S1), which confirmed that the radiointermediate product was synthesized successfully. The high radiochemical yield (85%) was obtained within 15 min synthesis time from the addition of [^{18}F]fluoride.

For the synthesis of [^{18}F]mBMFMB, even higher radiochemical yield (92%) was also obtained with a procedure similar to that of [^{18}F]BMFMB, instead of using 1,3-bis(bromomethyl)benzene as reactant. The analysis HPLC profiles are shown in Figure S2 (Supporting Information).

Preparation of [^{18}F]FMBTP and [^{18}F]mFMBTP. Based on the convenient labeling of radiointermediates, the total

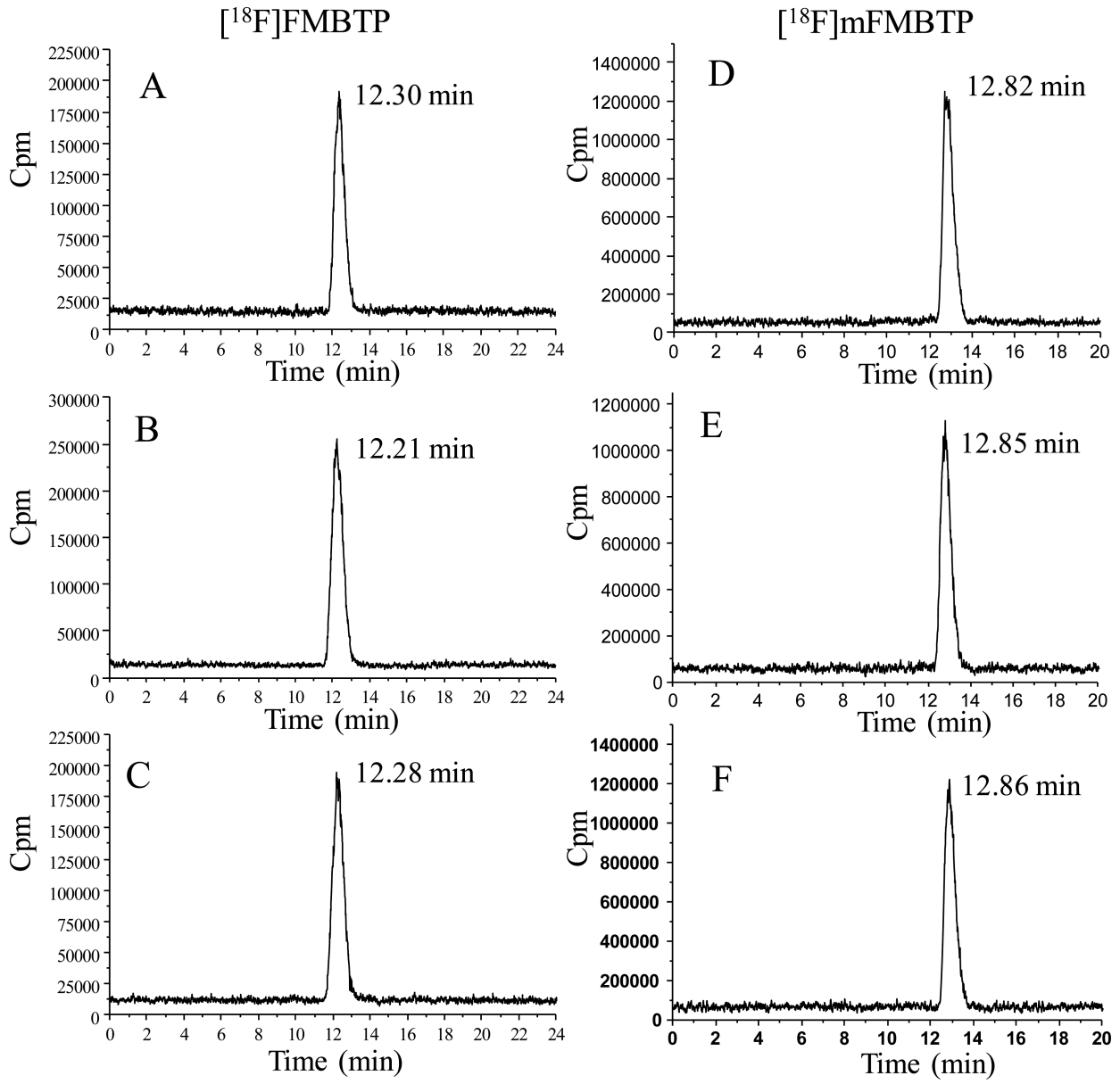

Figure 2. HPLC chromatograms of compounds [^{18}F]FMBTP (A) and [^{18}F]mFMBTP (D) and the profiles of stability study of [^{18}F]FMBTP and [^{18}F]mFMBTP after storage in water at room temperature for 3 h (B and E), and after incubation in murine plasma at 37 °C for 3 h (C and F) respectively. All the radiotracers were analyzed by using the isocratic HPLC method.

synthesis times of [^{18}F]FMBTP and [^{18}F]mFMBTP (from [^{18}F]fluoride) were about 50 and 55 min including HPLC purification, respectively. Their decay-corrected radiochemical yields were about 52 ± 9.3% (n = 7, for [^{18}F]FMBTP) and 50.6 ± 6.9% (n = 7, for [^{18}F]mFMBTP). The retention times of [^{18}F]FMBTP and [^{18}F]mFMBTP (12.30 and 12.82 min, respectively) also agreed well with the corresponding non-radioactive references [^{19}F]FMBTP and [^{19}F]mFMBTP (see Supporting Information: Figure S1 and S2). Both [^{18}F]FMBTP and [^{18}F]mFMBTP demonstrated excellent radiolabeling yields (>50%) and radiochemical purities (>99%). The specific activities of [^{18}F]FMBTP and [^{18}F]mFMBTP were estimated by HPLC analysis to be about 30 GBq/μmol and 38 GBq/μmol, respectively.

Physicochemical Property Study. The partition coefficients (log P) of [^{18}F]FMBTP and [^{18}F]mFMBTP were measured as 1.16 ± 0.003 (n = 3) and 1.05 ± 0.01 (n = 3), comparable to the [^{18}F]FETMP (1.27 ± 0.01)[28] and (6-[^{18}F]fluorohexyl)triphenylphosphonium salt ([^{18}F]3) (1.78 ± 0.05).[5] In paper electrophoresis, more than 98% [^{18}F]FMBTP and [^{18}F]mFMBTP were accumulated on the negative part, indicating that both of them were electropositive compounds.

For the in vitro stability studies, both of these radiotracers were intact in water solution (room temperature) and murine plasma (37 °C) after 3 h incubation (Figure 2), suggesting that they had very good stability *in vitro*.

***In Vitro* Cell Uptake Assays.** In this study, the binding abilities of [^{18}F]FMBTP, [^{18}F]mFMBTP, and [^{99m}Tc]sestamibi to the H9c2 cells (which have high mitochondrial membrane potential) and NIH/3T3 cells were evaluated and compared. For [^{18}F]FMBTP, cell uptake in H9c2 cells was much higher (>2.67-fold) than that in NIH/3T3 cells after incubation for 1 h. When the cells were pretreated with 1 μM CCCP for 0.5 h, cell uptake of [^{18}F]FMBTP was significantly inhibited to about

dx.doi.org/10.1021/mp500216g | *Mol. Pharmaceutics* 2014, 11, 3823−3831

70% ($P < 0.01$) (Figure 3). Analogously, cell uptake of [^{18}F]mFMBTP also higher (>1.52-fold) in H9c2 cells than that

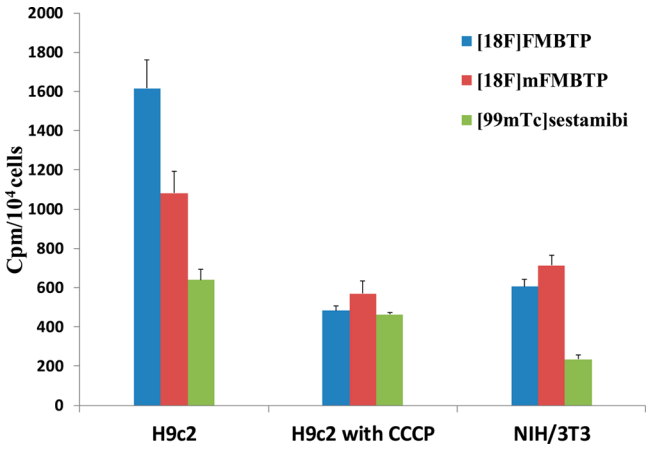

Figure 3. Cell uptake of [^{18}F]FMBTP, [^{18}F]mFMBTP, and [^{99m}Tc]-sestamibi in H9c2, H9c2 cells treated with 1 μM protonophore CCCP, and NIH/3T3 cells at 1.0 h in a 37 °C incubator.

in NIH/3T3 cells after incubation for 1 h. And the uptake in H9c2 cells could be inhibited to about 48% ($P < 0.01$) when pretreated with 1 μM CCCP for 0.5 h (Figure 3).

As a known membrane potential dependent tracer,[29] [^{99m}Tc]sestamibi was set as positive control. It had more than 2.7-fold higher uptake in H9c2 cells than that in NIH/3T3 cells after incubation for 1 h. And uptake of [^{99m}Tc]sestamibi in H9c2 cells was also obviously inhibited by 1 μM CCCP ($P < 0.01$) (Figure 3). These results fully demonstrate that the two novel ^{18}F-labeled cations reported here accumulate in the myocardial cells through the mitochondrial membrane potential, like [^{99m}Tc]sestamibi.

Biodistribution in Normal Mice. All the animal studies were carried out in compliance with relevant national laws relating to the conduct of animal experimentation.

The biological distribution results in mice are shown in Table 1. [^{18}F]FMBTP had high heart uptake (25.24 ± 2.97% ID/g at 5 min post injection, p.i.) and very good retention (28.99 ± 3.54% ID/g at 120 min p.i.). On the other hand, the clearance of [^{18}F]FMBTP from the nontarget tissues was very fast. For example, the liver uptake was decreased dramatically from 14.93 ± 1.46% ID/g (at 5 min p.i.) to 0.89 ± 0.29% ID/g (at 120 min p.i.). The heart-to-liver, heart-to-lung, and heart-to-blood ratios were 5.04, 5.80, and 32.9, respectively, at 30 min p.i., and increased to 32.5, 7.61, and 151.9, respectively, at 120 min p.i.

When compared with [^{18}F]FMBTP, [^{18}F]mFMBTP had higher heart uptake (31.02 ± 0.33% ID/g at 5 min p.i.) and better target-to-nontarget ratios at earlier time points, while at later time points, the heart uptake and target-to-nontarget ratios have no obviously difference. Both of these new cations have moderate muscle uptakes at all time points after injection (6.91 ± 1.04% ID/g for [^{18}F]FMBTP and 4.29 ± 0.67% ID/g for [^{18}F]mFMBTP at 60 min p.i., respectively) (Table 1), similar to that of previously reported lipophilic cations of [^{18}F]FPTP (6.16 ± 1.78% ID/g at 60 min p.i.)[10] and [^{18}F]3 (4.53 ± 0.54% ID/g at 60 min p.i.),[5] respectively. For all of the other tissues, these two radiotracers showed comparable radioactivity uptake except that [^{18}F]mFMBTP had less bone uptake at the later time points.

Above all, [^{18}F]mFMBTP seems to be promising as a potential myocardial perfusion imaging agent, this encourage us to further evaluate it by *in vivo* PET imaging in rat and dog.

MicroPET Imaging Studies. MicroPET studies using [^{18}F]mFMBTP showed an excellent image quality in rat at 5 min, 30 min, 60 min, and 120 min after iv injection. Decay corrected coronal images that contain the heart are shown in Figure 4; high contrast images were obtained with sustained high myocardium uptake and extremely low liver and lung uptake. From the time−activity curves derived from dynamic PET imaging (Figure 5), the highest myocardium uptake (SUV) was reached rapidly at very early time after injection and kept high across all time points to 120 min p.i. For liver uptake, it peaked at 5 min p.i. and was followed by rapid clearance. After 30 min p.i., it was even lower than that of lung uptake. Sustained low lung uptake was observed from about 2 min p.i. with SUV value of 0.5. The heart/liver ratio increased obviously due to the quick clearance from liver (1.37, 6.62, 12.06, and 18.64 at 5, 30, 60, and 120 min p.i., respectively). High heart/lung ratios (3.87, 5.39, 6.03, and 6.61 at 5, 30, 60, and 120 min p.i., respectively) were also obtained at all time points after injection. This agreed with the results of *ex vivo* biodistribution very well. It is worth mentioning that almost no bone uptake of [^{18}F]mFMBTP was observed in PET imaging, although high bone uptake was found in the biodistribution study of mice.

PET/CT Imaging in Dog. The representative whole-body 2D projection images of [^{18}F]mFMBTP in a healthy Beagle dog are shown in Figure 6. The heart could clearly be seen from 10

Table 1. Biodistribution Results of [^{18}F]FMBTP and [^{18}F]mFMBTP in Mice at 5, 30, 60, and 120 min after Injection (Expressed as % ID/g ± SD, $n = 5$)

	5 min		30 min		60 min		120 min	
organ	[^{18}F]FMBTP	[^{18}F]mFMBTP	[^{18}F]FMBTP	[^{18}F]mFMBTP	[^{18}F]FMBTP	[^{18}F]mFMBTP	[^{18}F]FMBTP	[^{18}F]mFMBTP
heart	25.24 ± 2.97	31.02 ± 0.33	26.08 ± 2.9	27.39 ± 1.46	31.17 ± 1.5	28.30 ± 2.36	28.99 ± 3.54	26.82 ± 3.46
liver	14.93 ± 1.46	14.94 ± 1.39	5.16 ± 0.64	6.29 ± 1.35	1.89 ± 0.32	2.39 ± 0.56	0.89 ± 0.29	1.02 ± 0.2
spleen	4.84 ± 0.87	5.75 ± 0.64	3.93 ± 0.83	6.09 ± 0.96	2.83 ± 0.51	3.83 ± 0.53	2.37 ± 0.55	2.41 ± 0.22
lung	6.53 ± 0.43	7.92 ± 0.34	4.49 ± 0.8	5.36 ± 0.68	4.1 ± 0.69	5.08 ± 0.32	3.81 ± 0.97	2.68 ± 0.46
muscle	5.35 ± 1.32	6.98 ± 1.14	4.95 ± 0.53	6.53 ± 1.65	6.91 ± 1.04	4.29 ± 0.67	5.81 ± 1.59	5.13 ± 0.3
bone	7.12 ± 1.42	6.59 ± 0.3	19.45 ± 1.93	18.13 ± 1.27	20.16 ± 3.9	14.2 ± 1.13	22.61 ± 5.5	11.69 ± 2.74
kidney	73.62 ± 5.4	51.11 ± 8.25	32.28 ± 1.63	36.22 ± 3.29	17.1 ± 3.72	19.73 ± 1.69	13.24 ± 1.31	11.04 ± 1.46
blood	1.82 ± 0.14	2.14 ± 0.16	0.79 ± 0.06	1.15 ± 0.14	0.41 ± 0.01	0.61 ± 0.05	0.19 ± 0.02	0.32 ± 0.05
heart/liver	1.69	2.08	5.04	4.84	16.43	11.84	32.5	26.25
heart/lung	3.86	3.91	5.80	5.11	7.46	5.57	7.61	9.97
heart/blood	13.87	14.44	32.90	23.82	74.74	46.39	151.90	83.98

dx.doi.org/10.1021/mp500216g | *Mol. Pharmaceutics* 2014, 11, 3823−3831

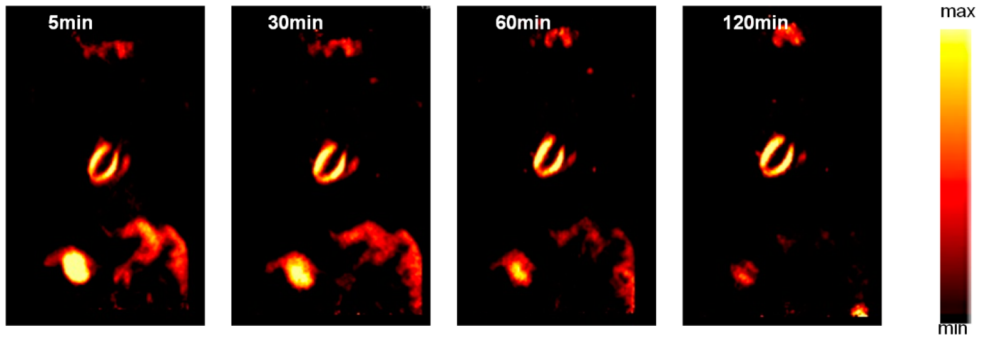

Figure 4. Coronal microPET images in normal rat. The heart was visible with excellent ratios of heart/liver and heart/lung, and fast clearance from small intestine at 5, 30, 60, and 120 min after iv injection of [^{18}F]mFMBTP, respectively.

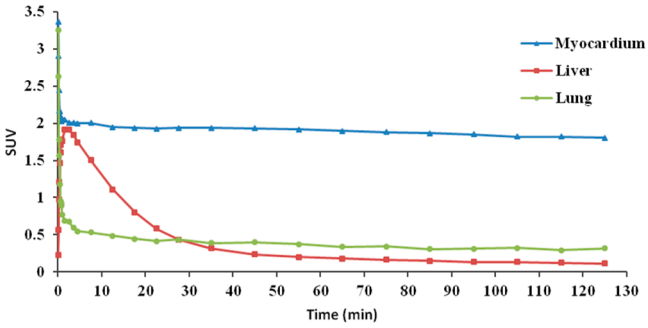

Figure 5. Time−activity curves generated from dynamic PET images. [^{18}F]mFMBTP accumulated specifically in the heart. The [^{18}F]-mFMBTP had excellent heart/liver and heart/lung ratios and in liver and lung was washed out rapidly but was retained in the myocardium for the whole time.

to 120 min after injection, and heart uptake had not obviously decreased. Radioactivity accumulated strongly in the kidney and gall bladder at all time points and gradually increased in the bladder from 10 to 120 min. Very low bone and muscle uptakes were observed from 30 min, and the heart-to-bone and heart-to-muscle ratios, which were derived from PET imaging, were 10.37, 13.16, 12.47, and 12.96 and 17.00, 17.74, 19.95, and 24.20 at 10, 30, 60, and 120 min after injection, respectively. Other organs and tissues had low background uptake because of the excellent metabolic properties of the compound. The heart/liver and heart/lung standardized uptake value ratios were calculated as 1.54 and 6.00 at 10 min after injection, 2.83 and 15.19 at 30 min after injection, 3.98 and 38 at 60 min after injection, and 7.76 and 35.28 at 120 min after injection, respectively. The results of PET imaging in dog were coincident with the biodistribution results in rat and mice.

DISCUSSION

The radiointermediates of [^{18}F]BMFMB and [^{18}F]mBMFMB had been reported previously by Vries et al.[24,25] In the literature, the radiointermediates were synthesized and purified with HPLC in approximately 55 min with low radiochemical yield (12% for [^{18}F]BMFMB and 26% for [^{18}F]mBMFMB), while in this study, the optimized labeling conditions were obtained with less precursor (3 mg) and Kryptofix 2.2.2 (2 mg) (see Supporting Information: Table S1). The radiochemical yields were increased significantly to 85% ([^{18}F]BMFMB) or 92% ([^{18}F]mBMFMB) by HPLC analysis with decay-correction, and the synthesis time was also shortened obviously to about 15 min (from [^{18}F]fluoride). Over all, the advantages of this highly efficient one-pot labeling method include smaller amounts of Kryptofix 2.2.2 and precursor, shorter synthesis time, and much higher radiochemical yield than that of previous study.

When compared with the previously reported phosphonium cations, [^{18}F]FMBTP and [^{18}F]mFMBTP have signicant advantages in the aspects of synthesis time and labeling yield due to the highly efficient one-pot labeling of radio-intermediate. For [^{18}F]FTPP, the synthesis time was reported as 120 min with 10% labeling yield.[23] For [^{18}F]FBnTP, it was synthesized in 82 min with only 6% radiochemical yield. Recently, Kim et al.[5] reported a new cation, (6-[^{18}F]-fluorohexyl)triphenylphosphonium salt ([^{18}F]3), which was prepared in a short time of 56 min while the radiochemical yield still needs to be improved (15−20%).

In this study, the preliminary properties and feasibilities of [^{18}F]FMBTP and [^{18}F]mFMBTP for myocardial perfusion imaging were investigated *in vitro* and *in vivo*. In the *ex vivo* bisdistribution study, both [^{18}F]FMBTP and [^{18}F]mFMBTP had comparable target/nontarget ratios to [^{18}F]FTPP and even

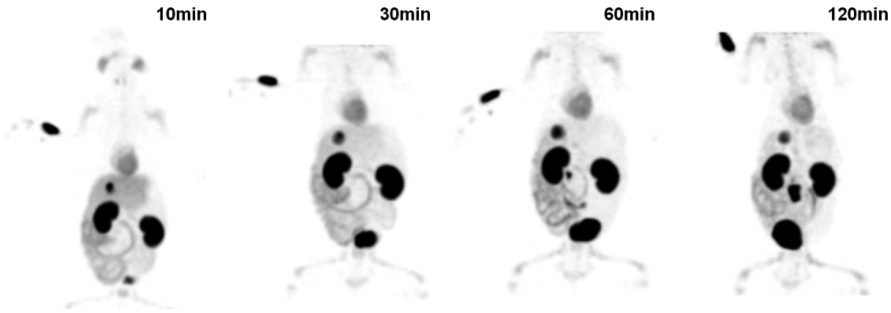

Figure 6. Whole-body 2D projection PET/CT images in normal Beagle dog at 10, 30, 60, and 120 min after iv injection of [^{18}F]mFMBTP, respectively.

dx.doi.org/10.1021/mp500216g | *Mol. Pharmaceutics* 2014, 11, 3823−3831

higher at later time points.[21] When compared to [^{18}F]-FETMP,[28] faster liver clearance for [^{18}F]FMBTP and [^{18}F]-mFMBTP was observed. The liver uptakes of [^{18}F]FETMP were 16.25 ± 2.77% ID/g at 10 min p.i. and 10.38 ± 1.94% ID/g at 120 min p.i., and only about 64% liver uptake was cleared after 2 h injection, obviously slower than that of both [^{18}F]FMBTP and [^{18}F]mFMBTP (more than 90% liver accumulation was cleared from 5 to 120 min p.i.).

The accumulation of activity in kidney may due to the electropositivity of [^{18}F]FMBTP and [^{18}F]mFMBTP, because kidney tubules have some compounds with negative charges which prefer to attract molecules with positive charges. Without doubt, the [^{18}F]FMBTP and [^{18}F]mFMBTP were excreted through kidney and finally washed out with urine. High bone uptakes were also found in mouse biodistribution for both [^{18}F]FMBTP and [^{18}F]mFMBTP, and the activity increased continuously with time for [^{18}F]FMBTP. The reason may due to the defluorination of tracers *in vivo* (see Supporting Information: Figure S3). Fortunately, there was no obvious bone uptake in the PET imaging in rat and dog.

In the study of [^{18}F]3, Kim et al.[5] claimed that highly lipophilic structures (such as benzene rings) should not be adopted for the radiolabeling of phosphonium salts because they could increase liver uptake. But in this study, although lipophilic structures were introduced as labeling intermediates in both [^{18}F]FMBTP and [^{18}F]mFMBTP, their liver uptake was cleared even much faster than that of [^{18}F]3. For instance, the liver uptake of [^{18}F]FMBTP was 5.16, 1.89, and 0.89% ID/g at 30, 60, and 120 min respectively, while that of [^{18}F]3 was 4.52, 3.70, and 2.84% ID/g at 30, 60, and 120 min, respectively. Furthermore, the introduction of the aromatic ^{18}F-labeling moiety does not increase the log *P* value of the tracers ([^{18}F]FMBTP and [^{18}F]mFMBTP have a log *P* similar to that of [^{18}F]FETMP[28] and [^{18}F]3[5]).

When compared with the previously reported phosphonium cations, these newly developed [^{18}F]FMBTP and [^{18}F]-mFMBTP had higher heart/liver ratio and lower lung uptake than those of [^{18}F]FBnTP[1,23] and [^{18}F]FTPP.[20,21] [^{18}F]FBnTP is metabolically stable and demonstrates excellent characteristics in healthy mice.[24] However, the slow liver clearance leads to low heart/liver ratio,[5] although a similar heart/liver ratio at 30 min had been reported for [^{18}F]FTPP[21] and [^{18}F]mFMBTP (this study), while the latter had much lower background uptake in PET imaging of rat. When compared to [^{18}F]FPTP,[10] the [^{18}F]mFMBTP reported here showed lower abdomen uptake at 30 and 60 min after injection.

In this study, [^{18}F]FMBTP and [^{18}F]mFMBTP were successfully prepared with high radiochemical yield 52 ± 9.3% (n = 7, for [^{18}F]FMBTP) and 50.6 ± 6.9% (n = 7, for [^{18}F]mFMBTP) and more than 99% of radiochemical purity. The mechanism of [^{18}F]FMBTP and [^{18}F]mFMBTP binding with myocardial cell was verified and compared with classic MPI agent [^{99m}Tc]sestamibi by *in vitro* cell uptake assays. At the same time, both [^{18}F]FMBTP and [^{18}F]mFMBTP displayed high uptake and good retention in the myocardium. [^{18}F]mFMBTP was further evaluated with PET imaging in rat and dog to give high-contrast heart images with rapid clearance from the liver, lung, and other organs. All of these preliminary data strongly imply that it may be a useful tool for myocardial perfusion imaging. The feasibility of [^{18}F]mFMBTP will be evaluated in animal myocardial infarction models, and the structure will be modified to lower bone uptake.

■ ASSOCIATED CONTENT

Supporting Information

NMR characterization, optimized radiolabeling conditions, HPLC analysis, urinary metabolites in mice, and biodistribution in rat. This material is available free of charge via the Internet at http://pubs.acs.org.

■ AUTHOR INFORMATION

Corresponding Author

*School of Public Health, Xiamen University, Xiang'an South Rd., Xiang'an district, Xiamen 361102, China. E-mail: zhangxzh@xmu.edu.cn. Phone: +86(592)2880645. Fax: +86(592)2880645.

Notes

The authors declare no competing financial interest.

‡First author. College of Chemistry, Beijing Normal University, 19 Xinjiekou Outer St., Beijing 100875, China. E-mail: 418zhaozuoquan@163.com. Phone: +8610-58802842. Fax: +8610-62208126.

■ ACKNOWLEDGMENTS

We thank Yuan Chen, Zhide Guo, Pu Zhang, Yi Sun, and Lin Wang for their generous help with biodistribution and PET imaging. This project was sponsored by the National Key Basic Research Program of China (2014CB744503) and the National Natural Science Foundation of China (21271030, 20871020, 81301251) and supported partially by Department of Nuclear Medicine of Peking Union Medical College Hospital.

■ REFERENCES

(1) Madar, I.; Ravert, H. T.; Du, Y.; Hilton, J.; Volokh, L.; Dannals, R. F.; Frost, J. J.; Hare, J. M. Characterization of uptake of the new PET imaging compound 18F-fluorobenzyl triphenyl phosphonium in dog myocardium. *J. Nucl. Med.* **2006**, *47*, 1359−1366.

(2) Mou, T.; Zhao, Z.; Fang, W.; Peng, C.; Guo, F.; Liu, B.; Ma, Y.; Zhang, X. Synthesis and preliminary evaluation of ^{18}F-labeled pyridaben analogues for myocardial perfusion imaging with PET. *J. Nucl. Med.* **2012**, *53*, 472−479.

(3) Mou, T.; Jing, H.; Yang, W.; Fang, W.; Peng, C.; Guo, F.; Zhang, X.; Pang, Y.; Ma, Y. Preparation and biodistribution of [^{18}F] FP2OP as myocardial perfusion imaging agent for positron emission tomography. *Bioorg. Med. Chem.* **2010**, *18*, 1312−1320.

(4) Gibbons, R. J.; Valeti, U. S.; Araoz, P. A.; Jaffe, A. S. The quantification of infarct size. *J. Am. Coll. Cardiol.* **2004**, *44*, 1533−1542.

(5) Kim, D. Y.; Kim, H. J.; Yu, K. H.; Min, J. J. Synthesis of [^{18}F]-labeled (6-fluorohexyl) triphenylphosphonium cation as a potential agent for myocardial imaging using positron emission tomography. *Bioconjugate Chem.* **2012**, *23*, 431−437.

(6) Knuuti, J.; Bengel, F. Positron emission tomography and molecular imaging. *Heart* **2008**, *94*, 360−367.

(7) Bateman, T. M. Cardiac positron emission tomography and the role of adenosine pharmacologic stress. *Am. J. Cardiol.* **2004**, *94*, 19−24.

(8) Siegrist, P. T.; Husmann, L.; Knabenhans, M.; Gaemperli, O.; Valenta, I.; Hoefflinghaus, T.; Scheffel, H.; Stolzmann, P.; Alkadhi, H.; Kaufmann, P. A. ^{13}N-ammonia myocardial perfusion imaging with a PET/CT scanner: impact on clinical decision making and cost-effectiveness. *Eur. J. Nucl. Med. Mol. Imaging* **2008**, *35*, 889−895.

(9) Sampson, U. K.; Dorbala, S.; Limaye, A.; Kwong, R.; Di Carli, M. F. Diagnostic accuracy of rubidium-82 myocardial perfusion imaging with hybrid positron emission tomography/computed tomography in the detection of coronary artery disease. *J. Am. Coll. Cardiol.* **2007**, *49*, 1052−1058.

(10) Kim, D.-Y.; Kim, H.-S.; Le, U. N.; Jiang, S. N.; Kim, H.-J.; Lee, K.-C.; Woo, S.-K.; Chung, J.; Kim, H.-S.; Bom, H.-S. Evaluation of a

mitochondrial voltage sensor,(^{18}F-fluoropentyl) triphenylphosphonium cation, in a rat myocardial infarction model. *J. Nucl. Med.* **2012**, *53*, 1779−1785.
(11) Kopka, K.; Schober, O.; Wagner, S. ^{18}F-labelled cardiac PET tracers: selected probes for the molecular imaging of transporters, receptors and proteases. *Basic Res. Cardiol.* **2008**, *103*, 131−143.
(12) Yu, M.; Guaraldi, M.; Kagan, M.; Mistry, M.; McDonald, J.; Bozek, J.; Yalamanchili, P.; Hayes, M.; Azure, M.; Purohit, A. Assessment of ^{18}F-labeled mitochondrial complex I inhibitors as PET myocardial perfusion imaging agents in rats, rabbits, and primates. *Eur. J. Nucl. Med. Mol. Imaging* **2009**, *36*, 63−72.
(13) Yu, M.; Guaraldi, M. T.; Mistry, M.; Kagan, M.; McDonald, J. L.; Drew, K.; Radeke, H.; Azure, M.; Purohit, A.; Casebier, D. S. BMS-747158−02: a novel PET myocardial perfusion imaging agent. *J. Nucl. Cardiol.* **2007**, *14*, 789−798.
(14) Nekolla, S. G.; Saraste, A. Novel ^{18}F-labeled PET myocardial perfusion tracers: bench to bedside. *Curr. Cardiol. Rep.* **2011**, *13*, 145−150.
(15) Huisman, M. C.; Higuchi, T.; Reder, S.; Nekolla, S. G.; Poethko, T.; Wester, H.-J.; Ziegler, S. I.; Casebier, D. S.; Robinson, S. P.; Schwaiger, M. Initial characterization of an ^{18}F-labeled myocardial perfusion tracer. *J. Nucl. Med.* **2008**, *49*, 630−636.
(16) Kronauge, J. F.; Chiu, M. L.; Cone, J. S.; Davison, A.; Holman, B. L.; Jones, A. G.; Piwnica-Worms, D. Comparison of neutral and cationic myocardial perfusion agents: characteristics of accumulation in cultured cells. *Int. J. Radiat. Appl. Instrum. B* **1992**, *19*, 141−148.
(17) Madar, I.; Ravert, H.; DiPaula, A.; Du, Y.; Dannals, R. F.; Becker, L. Assessment of severity of coronary artery stenosis in a canine model using the PET agent ^{18}F-fluorobenzyl triphenyl phosphonium: comparison with 99mTc-tetrofosmin. *J. Nucl. Med.* **2007**, *48*, 1021−1030.
(18) Min, J.-J.; Biswal, S.; Deroose, C.; Gambhir, S. S. Tetraphenylphosphonium as a novel molecular probe for imaging tumors. *J. Nucl. Med.* **2004**, *45*, 636−643.
(19) Madar, I.; Ravert, H.; Nelkin, B.; Abro, M.; Pomper, M.; Dannals, R.; Frost, J. J. Characterization of membrane potential-dependent uptake of the novel PET tracer ^{18}F-fluorobenzyl triphenylphosphonium cation. *Eur. J. Nucl. Med. Mol. Imaging* **2007**, *34*, 2057−2065.
(20) Cheng, Z.; Subbarayan, M.; Chen, X.; Gambhir, S. S. Synthesis of (4-[^{18}F] fluorophenyl) triphenylphosphonium as a potential imaging agent for mitochondrial dysfunction. *J. Labelled Compd. Radiopharm.* **2005**, *48*, 131−137.
(21) Shoup, T. M.; Elmaleh, D. R.; Brownell, A.-L.; Zhu, A.; Guerrero, J. L.; Fischman, A. J. Evaluation of (4-[^{18}F] Fluorophenyl) triphenylphosphonium ion. A potential myocardial blood flow agent for PET. *Mol. Imaging Biol.* **2011**, *13*, 511−517.
(22) Heinrich, T. K.; Gottumukkala, V.; Snay, E.; Dunning, P.; Fahey, F. H.; Ted Treves, S.; Packard, A. B. Synthesis of fluorine-18 labeled rhodamine B: A potential PET myocardial perfusion imaging agent. *Appl. Radiat. Isot.* **2010**, *68*, 96−100.
(23) Ravert, H. T.; Madar, I.; Dannals, R. F. Radiosynthesis of 3-[^{18}F] fluoropropyl and 4-[^{18}F] fluorobenzyl triarylphosphonium ions. *J. Labelled Compd. Radiopharm.* **2004**, *47*, 469−476.
(24) De Vries, E. F.; Vroegh, J.; Elsinga, P. H.; Vaalburg, W. Evaluation of fluorine-18-labeled alkylating agents as potential synthons for the labeling of oligonucleotides. *Appl. Radiat. Isot.* **2003**, *58*, 469−476.
(25) Namolingam, V.; Luthra, S.; Brady, F.; Pike, V. Radiosynthesis of 1-[^{18}F] fluoromethyl-4-methyl-benzene and a series of o-, m- or p-substituted 1-halomethyl-[^{18}F] fluoromethyl-benzenes. *J. Labelled Compd. Radiopharm.* **2001**, *44*, S917−S919.
(26) Steen, H.; Maring, J. G.; Meijer, D. K. Differential effects of metabolic inhibitors on cellular and mitochondrial uptake of organic cations in rat liver. *Biochem. Pharmacol.* **1993**, *45*, 809−818.
(27) Cheng, Z.; Winant, R. C.; Gambhir, S. S. A new strategy to screen molecular imaging probe uptake in cell culture without radiolabeling using matrix-assisted laser desorption/ionization time-of-flight mass spectrometry. *J. Nucl. Med.* **2005**, *46*, 878−886.
(28) Kim, D. Y.; Kim, H. J.; Yu, K. H.; Min, J. J. Synthesis of [^{18}F]-labeled (2-(2-fluoroethoxy) ethyl) tris (4-methoxyphenyl) phosphonium cation as a potential agent for positron emission tomography myocardial imaging. *Nucl. Med. Biol.* **2012**, *39*, 1093−1098.
(29) Zhou, Y.; Liu, S. ^{64}Cu-labeled phosphonium cations as PET radiotracers for tumor imaging. *Bioconjugate Chem.* **2011**, *22*, 1459−1472.